Positron and Electron Backscattering from Solids

G. R. Massoumi,(1) N. Hozhabri,(1) K. O. Jensen,(1) W. N. Lennard,(1) M. S. Lorenzo,(1) P. J. Schultz,(1) and A. B. Walker(1),(2)

(1)*Department of Physics, The University of Western Ontario, London, Ontario, Canada N6A 3K7*
(2)*School of Physics, University of East Anglia, Norwich NR4 7TJ, United Kingdom*
(Received 5 February 1992)

We present new experimental results for the angle and energy resolved backscattering of positrons and electrons from Al and Au at oblique incident angles. For e^+ incident on Au, and both e^- and e^+ incident on Al, evidence for specular scattering is observed. By contrast the e^- scattering from Au is nearly symmetric about the surface normal. For positrons we find excellent agreement between these data and Monte Carlo simulations based on the Penn dielectric function.

PACS numbers: 34.80.Bm, 25.30.Bf, 25.30.Hm, 34.90.+q

Backscattered positrons (or electrons) refer to those particles which, when directed towards a solid target at some incident energy, are scattered through more than 90° and returned into the vacuum. Although the definition is straightforward, a closer inspection reveals the process is in fact complex. What can be hidden in the simplicity is the extent of the physical interaction between projectile and target. It is clear that the backscattering process must be sensitively determined by the details of the elastic scattering interaction, but it is not clear to what extent inelastic processes determine the properties of the returning projectile. Even *less* is known about the interaction volume for the process. How deep does the typical positron or electron penetrate before returning to the surface? How much of the target material is traversed in the process? How many "collisions" contribute to the average backscattered particle, and what differences, if any, can be expected when matter (electron) and antimatter (positron) projectiles are interchanged?

Experimentally, the information lies in the full doubly-differential (i.e., angle and energy) distribution of backscattered particles. There is a relatively extensive literature base concerning experimental and theoretical studies of electron backscattering from thin films (see, for example, Niedrig's review and references therein) [1]. However, few investigations of differential electron backscattering for oblique incidence angles have been reported [2–6]. In addition, for positrons data are even more sparse [2,7]. Several semiempirical models have been advanced to describe electron backscattering [1], but the situation remains unsatisfactory for both theory and experiment.

In the present Letter, we describe the first doubly-differential e^- and e^+ backscattering measurements (i.e., $d^2\eta^{\pm}/dE\,d\Omega$) for monoenergetic particles (35 keV) incident on thick Au and Al targets. The angle of incidence was varied in the range $0° \leq \alpha \leq 80°$ relative to the sample normal ($\hat{\mathbf{n}}$), and scattered particle distributions were measured at different emission angles γ, using an energy dispersive surface barrier detector (SBD). The experiments were restricted to angles (γ) in the plane defined by the incident beam ($\hat{\mathbf{k}}$) and the sample normal ($\hat{\mathbf{n}}$).

Data for positrons are compared to Monte Carlo calculations, which are performed with *no* adjustable parameters, and the agreement is exceptionally good. This favorable comparison allows the detailed investigation of particle histories and the extrapolation of experimental results (restricted to a single scattering plane) to *all* emission angles. The backscattering distributions observed for 35-keV positrons on both Au and Al show a quasispecular component for large angles of incidence ($\alpha \geq 50°$). This feature is remarkable in light of the surprisingly large penetration depths (≈ 300 nm for Au and ≈ 1500 nm for Al) and number of collisions (≈ 300 and ≈ 400, respectively) determined from averages over those positrons which are backscattered.

Monoenergetic e^- and e^+ beams were obtained from the University of Western Ontario electrostatically guided positron beam facility. Positrons from a ^{58}Co source were moderated in solid Ar, focused by electrostatic lenses and accelerated to 35 keV. The electron beam was produced using a standard electron gun in place of the positron source. The beam intensities were kept to less than 10^4 Hz to facilitate single event counting. Other important features of the apparatus and experiment can be found in Refs. [7–9]. Tilt (α) and measurement (γ) angles are indicated in the inset of Fig. 1. Positive values of γ occur when the backscattered particles emerge on the opposite side of $\hat{\mathbf{n}}$ relative to the incident particles. The solid angle subtended by the SBD was $\Omega = 28$ msr, corresponding to a half angle of 5.4°.

In the Monte Carlo (MC) simulations [10], positron trajectories for a large number (typically $\sim 10^5$) of positrons were followed through the target material as they interacted with the target atoms via both elastic and inelastic processes. The inelastic scattering was described within the dielectric formalism: The doubly-differential cross section for a positron to undergo a scattering event is expressed in terms of $\mathrm{Im}(1/\epsilon)$, where $\epsilon(q,\omega)$ is the dielectric function for momentum transfer $\hbar q$ and energy loss $\hbar\omega$. The model dielectric function for $\mathrm{Im}(1/\epsilon)$ proposed by Penn [11] has been used; this function is a

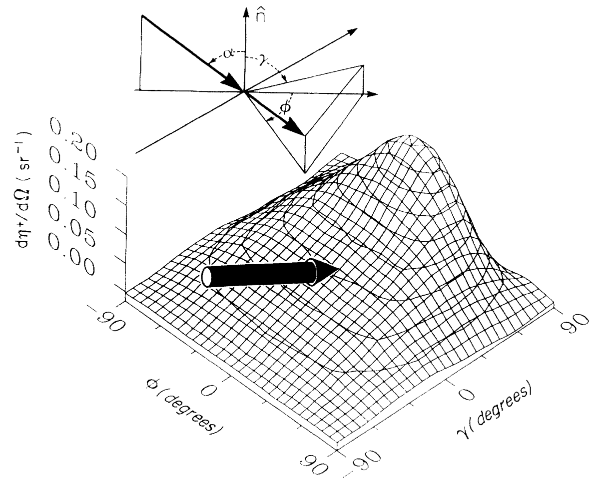

FIG. 1. Differential backscattering probability, $d\eta^+/d\Omega$, obtained from Monte Carlo simulations as a function of angles γ and ϕ (see the inset for geometry) for positrons incident on Al at an angle $\alpha=60°$. The arrow indicates the incident beam direction.

weighted average of Lindhard dielectric functions for different free-electron gas densities with a weight function derived from the optical dielectric function. The full dependence of the scattering cross sections on ω and q obtained from the Penn model are included in the simulations. The optical data were taken from Ref. [12], and using the full range of excitation energies from ~ 0.1 eV to several keV. Thus, the model accounts for both core and valence electron scattering including plasmon excitations. The elastic scattering is calculated using a partial wave expansion [13] where the atomic scattering potential was obtained from density-functional calculations within the local spin-density approximation. Since the Penn model ignores the indistinguishability of electrons, its applicability to electron-solid interactions is limited.

The simulations were performed for semi-infinite Al and Au targets having a planar surface. Those positrons returning to the surface with energy above 50 eV were considered to constitute the backscattered flux. The MC method used in this work has been applied to compute positron implantation depths in Al and Au, yielding excellent agreement with experiment [14].

Figure 1 shows a three-dimensional representation of the MC results for $d\eta^+/d\Omega$ (integrated over energy) for 35 keV e^+ incident on a thick Al target at $\alpha=60°$. A pronounced but broadened specular peak is clearly evident at low values of ϕ. For larger angles ($\phi \to 90°$), the distribution becomes increasingly symmetric around the surface normal ($\gamma=0°$).

Figure 2(a) shows e^+ angular backscattering distributions at $\phi=0°$ for both Au and Al targets for $\alpha=60°$. The specular reflection peak near $\gamma \approx \alpha$ is apparent, especially for the Al target. The agreement between MC and experiment is better than 5% everywhere, which is particularly encouraging since there are no adjustable parameters. The excellent agreement invites a more detailed investigation of particle history, as shown in Figs. 2(b) and 2(c). We note that backscattered positrons have experienced hundreds of collisions and penetrated hundreds of nanometers normal to the surface even for this large angle of incidence. Remarkably, the broad specular component for Al is dominated by those positrons having a mean penetration depth of ~ 300 nm. A similar feature has already been observed in the electron backscattered distribution from low-Z bulk materials as early as 1957 [3]. However, the new results presented here contradict previous suggestions that the specular component arises from incident projectiles that have not penetrated far into the solid.

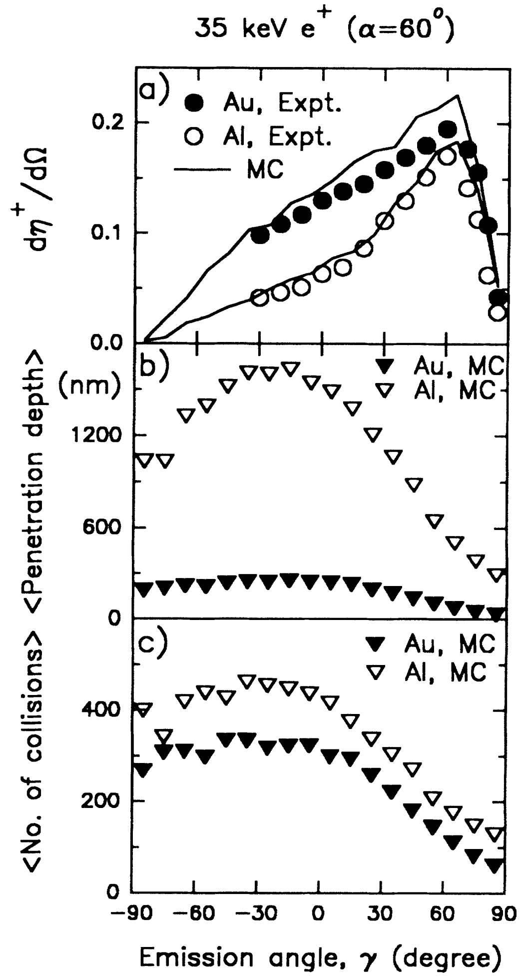

FIG. 2. (a) Experimental and calculated MC angular backscattering distributions, $d\eta^+/d\Omega$, as a function of angle, γ, for the $\phi=0°$ plane for positrons incident at an angle $\alpha=60°$. (b) Calculated mean penetration depth (normal to the surface) reached by backscattered positrons as a function of the emission angle, γ. (c) Calculated mean number of collisions for backscattered positrons at different emission angles, γ.

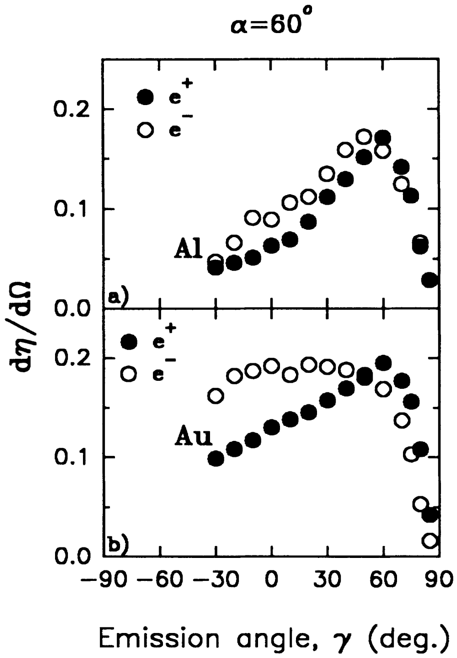

FIG. 3. Experimental differential backscattering probabilities as a function of emission angle, γ, for positrons and electrons incident at $\alpha = 60°$ on (a) Al and (b) Au thick targets.

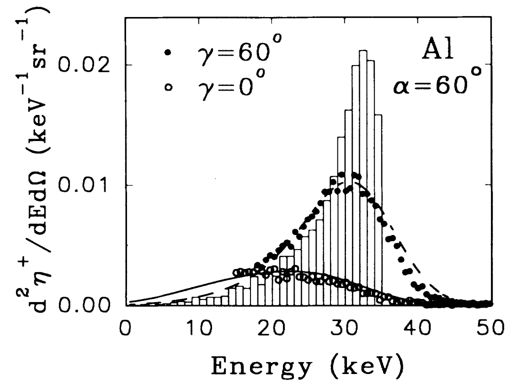

FIG. 4. Energy spectra of backscattered positrons, corresponding to the doubly-differential backscattering probabilities, $d^2\eta/dE\,d\Omega$, for incident angle $\alpha = 60°$ on Al and emission angles $\gamma = 0°$ and 60°. Circles denote the experimental results; the smooth curves show the Monte Carlo results convoluted with the energy resolution of the detector. The histogram shows the Monte Carlo results for $\gamma = 60°$ before convolution.

Figure 3 shows experimental results for $d\eta/d\Omega$ for both positrons and electrons incident at $\alpha = 60°$. For Au, the specular distribution observed for positrons contrasts sharply with the angular distribution of backscattered electrons, which is nearly symmetric about the surface normal. This observation provides significant experimental evidence for a fundamental difference in the elastic and inelastic cross sections for electrons and positrons. Such differences are expected to increase with increasing Z for energies exceeding a few keV [15]. However, since the backscattered distributions result from a large number of binary collisions, it is not easy to predict the angular dependence of e^+-e^- differences. Our electron data for Al and Au are in satisfactory agreement with earlier measurements. Thus, it is the presence of the quasispecular behavior for e^+ incident on *both* Al and Au that is surprising. Nevertheless, repeated measurements have confirmed the results shown in Figs. 2 and 3, which have (for e^+) been convincingly supported by calculations. It will be interesting to see if the extension of Monte Carlo calculations to e^- can account for the experimentally measured distributions.

Finally, we show in Fig. 4 two examples of the full doubly-differential positron scattering distributions, $d^2\eta/dE\,d\Omega$, for Al at $\alpha = 60°$. The solid curves are the MC results after convolution with a 12-keV Gaussian to account for the energy resolution of the SBD. Again, the excellent agreement lends confidence to the Monte Carlo histogram, shown for the $\gamma = 60°$ case only. This result illustrates the sharply peaked elasticlike scattering which dominates in all cases.

In conclusion, we have presented doubly-differential backscattering data for positrons and electrons incident on thick elemental targets at 35 keV. The results clearly illustrate significant differences for e^- and e^+, particularly, for high-Z targets. The excellent agreement between data and calculations for positrons suggests that both the transport model and the scattering cross sections used in the simulations are reliable. In particular, the present results and the earlier agreement with experimental positron implantation depths [14] confirm the accuracy of the Penn dielectric model [11] for inelastic scattering of *positrons*. Two important observations are evident from the present study. The first is the surprising depth of penetration for backscattered e^+. In the case of Al, the mean penetration depth was ≈ 300 nm, while the average of the *maximum* penetration depth [shown in Fig. 2(b)] was in excess of 1500 nm. The second remarkable observation is the quasispecular feature observed for both e^+ and e^- scattered from Al, and for e^+ scattered from Au, which is even more surprising in light of the penetration depths noted above. The reason for the Al/Au difference in scattering e^+ vs e^- remains unsolved, although more extensive measurements and e^- Monte Carlo calculations presently underway may help to resolve this issue.

Funding for this research has been provided by the National Sciences and Engineering Research Council (NSERC) of Canada (W.N.L., P.J.S.) and from the Network of Centres of Excellence in Molecular and Interfacial Dynamics, one of the fifteen Networks of Centres of Excellence supported by the Government of Canada (N.H., K.O.J., P.J.S.).

[1] H. Niedrig, J. Appl. Phys. **53**, R1 (1982).

[2] H. H. Seliger, Phys. Rev. **88**, 408 (1952).
[3] H. Kanter, Ann. Phys. (N.Y.) **6**, 144 (1957).
[4] G. Neubert and S. Rogaschewski, Phys. Status Solidi (a) **59**, 35 (1980).
[5] L. Reimer, W. Pöpper, and W. Bröcker, Scanning Electron Microsc. **1**, 705 (1978).
[6] A. Darlinski, Phys. Status Solidi (a) **63**, 663 (1981).
[7] G. R. Massoumi, N. Hozhabri, W. N. Lennard, and P. J. Schultz, Phys. Rev. B **44**, 3486 (1991).
[8] G. R. Massoumi, N. Hozhabri, W. N. Lennard, P. J. Schultz, S. F. Baert, H. H. Jorch, and A. H. Weiss, Rev. Sci. Instrum. **62**, 1460 (1991).
[9] G. R. Massoumi, W. N. Lennard, H. H. Jorch, and P. J. Schultz, in *Positron Beams for Solids and Surfaces*, edited by P. J. Schultz, G. R. Massoumi, and P. J. Simpson, AIP Conf. Proc. No. 218 (AIP, New York, 1990), p. 39.
[10] Full details of the Monte Carlo simulation method will be described in a forthcoming publication: K. O. Jensen and A. B. Walker (unpublished).
[11] D. R. Penn, Phys. Rev. B **35**, 482 (1987).
[12] *Handbook of Optical Constants of Solids*, edited by E. D. Palik (Academic, Orlando, 1985).
[13] K. O. Jensen, A. B. Walker, and N. Bouarissa, in *Positron Beams for Solids and Surfaces* (Ref. [9]).
[14] J. A. Baker, N. B. Chilton, K. O. Jensen, A. B. Walker, and P. G. Coleman, Appl. Phys. Lett. (to be published).
[15] P. J. Schultz, L. R. Logan, W. N. Lennard, and G. R. Massoumi, Scanning Microsc. Suppl. **4**, 223 (1990).